

International Journal of Engineering Sciences & Research Technology

(A Peer Reviewed Online Journal)
Impact Factor: 5.164



Chief Editor

Dr. J.B. Helonde

Executive Editor

Mr. Somil Mayur Shah

ABSTRACT

The aim of this study is to provide an analysis on pollutant concentration in surface waters using one – dimensional advection diffusion equation with temporally varying coefficients. Numerical and analytical solutions are obtained for one - dimensional Advection Diffusion Equations with variable coefficients in a finite medium. Finite Difference and Laplace Transforms Methods are applied to solve the Advection Diffusion Equation with temporally varying coefficients. Absolute error obtained from comparing analytical and numerical solutions at different points reveals that the numerical scheme is accurate. Simulations based on the validated numerical scheme are obtained. Simulations on the effect of dispersion and velocity coefficients (based on Peclet number) on pollutant concentration show that concentration increases around the source point and gradually decreases with increasing distance from the source point. It further shows that concentration is higher for Peclet number much greater than one as compared to Peclet numbers much less than or equal to one. Effect of temporally varying velocity and dispersion coefficients on pollutant concentration is also presented. The findings show that concentration is higher for exponentially decreasing dispersion in an exponentially accelerating flow and lower for exponentially increasing dispersion in an exponentially accelerating flow.

KEYWORDS: Advection Diffusion Equation, Finite Difference Method

1. INTRODUCTION

The transport of pollutants in natural streams such as rivers may be as a result of two processes namely dispersion and advection. These processes are prescribed in a mathematical model (Advection Diffusion Equation) that describes how pollutants are transported from one region to another. The Advection Diffusion Equation (ADE) is a parabolic partial differential equation based on conservation of mass and Fick's first law. It distinguishes two transport modes; the advective transport as a result of pollutant molecules being carried by the bulk motion of the fluid and transport due to hydrodynamic dispersion. Hydrodynamic dispersion is the combination of molecular diffusion and mechanical dispersion. The effects of advection and hydrodynamic dispersion in transportation of pollutant molecules are represented in the ADE as advection and dispersion coefficients. The velocity and dispersion coefficients of the ADE may be considered to be constant, spatially varying, temporally varying, or spatially and temporally varying. In this study, temporally varying velocity and dispersion coefficients are considered. Solutions of partial differential equations that describe transport processes have been obtained in various studies using numerical methods such as Finite Difference Method (FDM), Finite Element Method (FEM) and Finite Volume Method (FVM).

Andallah & Khatun (2020) obtained a numerical solution for the one - dimensional ADE using explicit centered difference and Crank Nicolson schemes (CNS) for a prescribed initial condition. They established that Crank Nicolson scheme is unconditionally stable using von Neumann stability criterion. They further performed error estimation of forward time central space, centered scheme (FTCSCS), forward time backward space, centered space (FTBSCS) and Crank Nicolson schemes to determine the accuracy and rate of convergence of these three

schemes. They observed that Crank Nicolson scheme is the most accurate scheme and that FTCSCS and CNS show good rate of convergence. An analytical and numerical solution of a one - dimensional ADE with uniformly and exponentially increasing forms of sources was determined by Manitcharoen & Pimpunchat (2020). Laplace transforms was used to solve the ADE with constant coefficients; and explicit finite difference techniques to solve the ADE with spatially varying coefficients. Numerical approximations were compared against relative error values. They concluded that the analytical and numerical solutions agreed to a higher degree. Alebrahim (2017) applied Forward Time Centered Space (FTCS) to solve a non - trivial transport problem using different time step (Δt) and space size (Δx). While imposing Dirichlet boundary conditions, it was observed that the results were converging to the exact solution if dispersion coefficient, Δt and Δx are small. Ahmed (2012) developed a new Finite Difference scheme based on mathematical combination between Siemieniuch and Gradwell approximations for time and Dehgans approximation for spatial differences. The new scheme was used to determine the numerical solution for a one - dimensional ADE with constant and variable coefficients. The numerical solutions were compared with some available analytical solutions and showed a good agreement. Tenth order Finite Difference Scheme in space and a fourth order Runge kutta scheme in time was applied by Gurarslan et al (2010) to solve a one - dimensional ADE. Numerical experiments demonstrated that the schemes were efficient and had higher order accuracy for $Pe \leq 5$. Yip (2021) studied pollutant transport in a straight narrow channel using upwind finite difference method. They used explicit, backward and central differences to discretize the time scale, the advection term and the diffusion terms respectively. The numerical model was validated against an existing analytical solution and the results showed good agreement between the analytical and numerical solutions. The validated model was applied to different cases of pollutant release mechanisms involving continuous and instantaneous pollutant releases, further observing that this model could capture the physics of the problem and be able to provide valuable information on the time and spatial evolution of pollutant concentration in both cases. When comparing the performance of the forward time centered space and the Crank Nicolson schemes for advection diffusion equation with various velocity and dispersion parameters, Johari et al (2018) observed that Crank Nicolson schemes were better than the forward time centered space in terms of accuracy. A numerical solution of the one dimensional ADE using standard and non - standard finite difference schemes was also obtained by Appadu (2013). The researcher used explicit Lax Wendroff, Crank Nicolson and a non - standard scheme to determine the solution to the ADE subject to specified initial and boundary conditions. It was observed that Crank Nicolson method was the most efficient method followed by the non - standard finite difference scheme. In a study aimed at comparing the accuracy of four numerical methods in solving a one-dimensional ADE, Kaya & Gharehbaghi (2014) used Finite Difference Method (FDM), Fourth Order Finite Difference Method (FOFDM), Finite Volume Method (FVM) and Differential Quadrature Method (DQM) in implicit conditions. They deduced that DQM provided better accurate results followed by FOFDM. FDM produced worst results. Huang et al (1997) on the other hand developed a third order numerical scheme with upwind weighting for solving the solute transport equation. This scheme yielded very accurate solutions near sharp concentration fronts, thereby showing its ability to eliminate numerical dispersion. However, the scheme was found to suffer from numerical oscillations, and could be avoided by employing upwind weighting techniques in the numerical scheme. Solutions obtained after upwind weighting were free of numerical oscillations and exhibited negligible numerical dispersion.

In most studies on numerical solution of one - dimensional ADE we encountered, researchers have used FDM to solve the ADE with constant coefficients subject to various initial and boundary conditions. Though Ahmed (2012) considered spatially varying dispersion and velocity coefficients, their study did not explore temporally varying coefficients. Our current study determines pollutant concentration using Finite Difference Method with discretization based on forward time central space, centered scheme (FTCSCS).

2. MATERIALS AND METHODS

Modeling and simulation of pollutant concentration from a point source into surface waters can be broken down into the following steps: Formulation of the model (describing the geometry of the domain, introducing sources, sinks and dispersion characteristics of the entire domain, introducing the appropriate boundary conditions), solving the model using finite differences and simulation of results. In our study, both numerical and analytical solutions of the model have been determined. Analytical solutions are obtained to validate the numerical results. Simulation of results based on the validated numerical results is presented.

2.1 Model Formulation

[http:// www.ijesrt.com](http://www.ijesrt.com) © International Journal of Engineering Sciences & Research Technology

[2]



Transport of pollutants in rivers is commonly described using processes of advection and diffusion. Based on the assumptions that: The flow conditions are unsteady; transport dominantly occurs along the longitudinal direction; pollutants are soluble compounds which may be subjected to advection and diffusion processes, pollutants are conservative in nature and pollutants emanate from discrete locations, the process of transportation of pollutants in surface waters is mathematically described using Advection - Diffusion Equation (ADE)

$$\frac{\partial c(x,t)}{\partial t} - D(x,t) \frac{\partial^2 c(x,t)}{\partial x^2} + U(x,t) \frac{\partial c(x,t)}{\partial x} = \lambda(t) \delta(x - S) \quad (1)$$

Where $c(x,t)$ is the pollutant concentration. $D(x,t)$ and $U(x,t)$ are the dispersion and velocity coefficients respectively. $\lambda(t) \delta(x - S)$ represents the source term where $\lambda(t)$ is the source intensity and $\delta(x - S)$ is a function that mathematically represents a point source. Here S is pollutant source location and δ is Dirac delta function. In our study, both dispersion and velocity coefficients are dependent on time only thus the pollutant dispersion and velocity parameters in Equation (1) can be written in terms of initial dispersion D_0 and uniform velocity coefficients U_0 as

$$D(t) = D_0 f_1(mt) \quad (2)$$

$$U(t) = U_0 f_2(mt) \quad (3)$$

Where $f_i(mt), i = 1, 2$ is a function that describes the temporal dependence of the velocity and dispersion coefficients, m is the unsteady parameter whose dimension is inverse of time variable t . Substituting Equations (2) and (3) in Equation (1) yields

$$\frac{\partial c(x,t)}{\partial t} - D_0 f_1(mt) \frac{\partial^2 c(x,t)}{\partial x^2} + U_0 f_2(mt) \frac{\partial c(x,t)}{\partial x} = \lambda(t) \delta(x - S) \quad (4)$$

But $\delta(x - S) = 0$ for $x \neq S$ (Duffy, 2001), Equation (4) becomes

$$\frac{\partial c(x,t)}{\partial t} - D_0 f_1(mt) \frac{\partial^2 c(x,t)}{\partial x^2} + U_0 f_2(mt) \frac{\partial c(x,t)}{\partial x} = 0 \quad (5)$$

Further assuming that no pollution has occurred at some initial time; there is a continuous mass injection of pollutants at the point $x = 0$ and that there is zero concentration gradient at the downstream. The initial and boundary conditions used include

$$c(x, 0) = 0; 0 \leq x \leq l; t > 0 \quad (6)$$

$$c(0, t) = C_0; t > 0 \quad (7)$$

$$\frac{\partial c(L,t)}{\partial x} = 0; t > 0 \quad (8)$$

2.2 Solution of Mathematical Model

We start by rewriting Equations (5) – (8) in non – dimensional form. We use the following dimensionless quantities:

$$c^* = \frac{c}{C_0}; t^* = \frac{tD_0}{L^2}; x^* = \frac{x}{L}; Pe = \frac{LU_0}{D_0} \quad (9)$$

Where C_0 is the input concentration, L is the length scale of the spatial domain, t^* is the time scale and Peclet number (Pe) is the ratio of advective and diffusive fluxes. Applying the dimensionless quantities in Equation (9) on Equation (5) yields

$$\frac{\partial c^*}{\partial t^*} = f_1(mt^*) \frac{\partial^2 c^*}{\partial x^{*2}} - Pe f_2(mt^*) \frac{\partial c^*}{\partial x^*} \quad (10)$$

Non – dimensionalizing the initial and boundary conditions in Equations (6) – (8) yields

$$c^* = 0; t^* = 0 \tag{11}$$

$$c^* = 1; x^* = 0 \tag{12}$$

$$\frac{\partial c^*}{\partial x^*} = 0; x^* = l \tag{13}$$

Numerical and analytical solutions of Equations (10) – (13) are determined.

2.2.1 Numerical Solution

Finite difference method is applied to solve the dimensionless Equation (10) subject to the initial and boundary conditions in Equations (11) – (13). We discretize the domain by dividing the solution domain in the xt - plane into equal meshes with grid points, each mesh with step size Δx^* by Δt^* . The interval $[0, l]$ is divided into n equal parts by the points $x_1^*, x_2^*, \dots, \dots, x_{n+1}^*$ with step length $\Delta x^* = \frac{x_{n+1}^* - x_1^*}{n}$. Similarly, the time interval is divided into m equal parts by the points $t_1^*, t_2^*, \dots, \dots, t_{m+1}^*$ with time step $\Delta t^* = \frac{t_{m+1}^* - t_1^*}{m}$. We compute $c^*(x_i, t_j)$ for $i = 1, 2, \dots, n + 1; j = 1, 2, \dots, m + 1$. We then approximate the difference equation into finite difference equations. Using Taylor series expansion for the first and second order derivatives, the combination gives rise to either Explicit or Implicit schemes. In this study, an explicit centered difference scheme (Forward time Central Space, Centered Scheme (FTCSCS)) is used to determine the solution. Discretization of time and space derivatives of c^* in Equation (10) using FTCSCS at $(i, j)^{th}$ node is given by

$$\frac{\partial c^*}{\partial t^*} = \frac{c_i^{*j+1} - c_i^{*j}}{\Delta t^*} \tag{14}$$

$$\frac{\partial c^*}{\partial x^*} = \frac{c_{i+1}^{*j} - c_{i-1}^{*j}}{2\Delta x^*} \tag{15}$$

$$\frac{\partial^2 c^*}{\partial x^{*2}} = \frac{c_{i-1}^{*j} - 2c_i^{*j} + c_{i+1}^{*j}}{\Delta x^{*2}} \tag{16}$$

Substituting Equations (14) - (16) in Equation (10) gives:

$$c_i^{*j+1} = c_i^{*j} + \Delta t^* f_1^j \left[\frac{c_{i-1}^{*j} - 2c_i^{*j} + c_{i+1}^{*j}}{\Delta x^{*2}} \right] - \Delta t^* f_2^j Pe \left[\frac{c_{i+1}^{*j} - c_{i-1}^{*j}}{2\Delta x^*} \right] \tag{17}$$

Let $\gamma = \frac{\Delta t^*}{\Delta x^{*2}}$ (18)

Let $\vartheta = \frac{Pe\Delta t^*}{\Delta x^*}$ (19)

Rewriting Equation (17) using Equations (18) and (19), then rearranging it according to the time levels on c^* gives:

$$c_i^{*j+1} = \left(\gamma f_1^j + \frac{\vartheta f_2^j}{2} \right) c_{i-1}^{*j} + (1 - 2\gamma f_1^j) c_i^{*j} + \left(\gamma f_1^j - \frac{\vartheta f_2^j}{2} \right) c_{i+1}^{*j} \tag{20}$$

Let

$$\delta = \gamma f_1^j + \frac{\vartheta f_2^j}{2}; \beta = 1 - 2\gamma f_1^j; \alpha = \gamma f_1^j - \frac{\vartheta f_2^j}{2} \tag{21}$$

Rewriting Equation (20) using Equation (21) gives:



$$c_i^{*j+1} = \delta c_{i-1}^{*j} + \beta c_i^{*j} + \alpha c_{i+1}^{*j} \tag{22}$$

Equation (22) is used for the interior nodes. The initial condition in Equation (11) is discretized as

$$c_i^{*0} = c^*(x_i^*, 0) = 0 \tag{23}$$

The discretized inlet boundary condition in Equation (12) is given by

$$c_1^{*j+1} = 1 \tag{24}$$

To discretize the boundary condition in Equation (13) at $i = n$, we introduce a ghost boundary node x_{n+1}^* and its corresponding approximation as $c_{n+1}^{*j} = c^*(x_{n+1}^*, t_j^*)$. Then using Equation (13) and the central difference formula in Equation (15) at the last boundary (x_n^*), we get

$$c_{n+1}^{*j} = c_{n-1}^{*j} \tag{25}$$

Rewriting Equation (22) using $i = n$

$$c_n^{*j+1} = \delta c_{n-1}^{*j} + \beta c_n^{*j} + \alpha c_{n+1}^{*j} \tag{26}$$

Applying Equation (25) on Equation (26) gives:

$$c_n^{*j+1} = (\alpha + \delta)c_{n-1}^{*j} + \beta c_n^{*j} \tag{27}$$

Equation (27) is the discretized equation of boundary condition in Equation (13). Using Equations (24), (22) and (27), the governing equation and the boundary conditions is expressed as a system of linear equations:

$$\left. \begin{aligned} c_1^{*j+1} &= 1 \\ c_i^{*j+1} &= \delta c_{i-1}^{*j} + \beta c_i^{*j} + \alpha c_{i+1}^{*j} \quad \text{for } i = 2, \dots, n \\ c_n^{*j+1} &= (\alpha + \delta)c_{n-1}^{*j} + \beta c_n^{*j} \end{aligned} \right\} \tag{28}$$

The solution to Equation (28) is obtained iteratively. To ensure stability of the scheme, the parameters $0 \leq \vartheta \leq \frac{1}{Pe}$ and $0 \leq \gamma \leq \frac{1}{2}$ (Andallah L.S. and Khatun, (2020)) are used. ϑ and γ are defined in Equations (18) and (19) respectively.

2.2.2 Analytical Solution

Analytical solution of Equation (10) subject to the initial and boundary conditions in Equations (11) – (13) is determined. Our solution is the dimensionless form of the solution obtained by Kumar *et al* (2011) for input concentration $C_0 = 1$. Consider the transformation

$$X^* = x \frac{f_2(mt^*)}{f_1(mt^*)} \tag{29}$$

Rewriting Equation (10) using Equation (29) gives

$$\frac{f_1}{f_2^2} \frac{\partial c^*}{\partial t^*} = \frac{\partial^2 c^*}{\partial X^{*2}} - Pe \frac{\partial c^*}{\partial X^*} \tag{30}$$

Introducing a new time variable using the transformation

$$T^* = \int_0^{t^*} \frac{f_2^2}{f_1} d\tau \tag{31}$$

Rewriting Equation (30) using Equation (31) gives



$$\frac{\partial c^*}{\partial T^*} = \frac{\partial^2 c^*}{\partial X^{*2}} - Pe \frac{\partial c^*}{\partial X^*} \quad (32)$$

Transforming the initial and boundary conditions in Equations (11) – (13) yields

$$c^*(X^*, 0) = 0 \quad (33)$$

$$c^*(0, T^*) = 1 \quad (34)$$

$$\frac{\partial c^*(L, T^*)}{\partial X^*} = 0 \quad (35)$$

Further application of the transformation

$$c^*(X^*, T^*) = K^*(X^*, T^*) \exp\left(\frac{Pe}{2}X^* - \frac{Pe^2}{4}T^*\right) \quad (36)$$

to eliminate $\frac{\partial c^*}{\partial X^*}$ in Equation (32) gives a diffusion equation

$$\frac{\partial K^*}{\partial T^*} = \frac{\partial^2 K^*}{\partial X^{*2}} \quad (37)$$

Transforming Equations (33) – (35) using Equation (36)

$$K^*(X^*, 0) = 0 \quad (38)$$

$$K^*(0, T^*) = e^{\mu T^*}; \mu = \frac{Pe^2}{4} \quad (39)$$

$$\frac{\partial K^*}{\partial X^*} + \frac{Pe}{2}K^* = 0 \quad (40)$$

Applying Laplace transforms to Equations (37) – (40) produces

$$\frac{d^2 \bar{K}^*}{dX^{*2}} - p\bar{K}^* = 0 \quad (41)$$

$$\bar{K}^*(0, p) = \frac{1}{p - \mu} \quad (42)$$

$$\frac{d\bar{K}^*}{dX^*} + \frac{Pe}{2}\bar{K}^* = 0 \quad (43)$$

Where $\bar{K}^*(X^*, p) = L[K^*(X^*, T^*)] = \int_0^\infty K^*(X^*, T^*)e^{-pT^*} dT^*$

The particular solution to Equations (41) – (43) is obtained as

$$\bar{K}^*(X^*, p) = \frac{1}{p - \mu} e^{-\sqrt{p}X^*} \quad (44)$$

Applying Laplace inverse on Equation (44) using the tables in Van and Alves (1982) gives the solution to our diffusion equation as

$$K^*(X^*, T^*) = \frac{1}{2} \left[\exp\left(\frac{Pe^2 T^*}{4} - \frac{Pe X^*}{2}\right) \operatorname{erfc}\left(\frac{X^*}{2\sqrt{T^*}} - \frac{Pe\sqrt{T^*}}{2}\right) + \exp\left(\frac{Pe^2 T^*}{4} + \frac{Pe X^*}{2}\right) \operatorname{erfc}\left(\frac{X^*}{2\sqrt{T^*}} + \frac{Pe\sqrt{T^*}}{2}\right) \right] \quad (45)$$

Inserting Equation (45) in Equation (36) and further applying Equations (29) and (31) gives the analytical solution to the model:

$$c^*(x^*, t^*) = \frac{1}{2} \left[\operatorname{erfc}\left(\frac{x f_2(mt^*)}{2\sqrt{T^*} f_1(mt^*)} - \frac{Pe\sqrt{T^*}}{2}\right) + \exp\left(x \frac{f_2(mt^*)}{f_1(mt^*)} Pe\right) \operatorname{erfc}\left(\frac{x f_2(mt^*)}{2\sqrt{T^*} f_1(mt^*)} + \frac{Pe\sqrt{T^*}}{2}\right) \right] \quad (46)$$

3. RESULTS AND DISCUSSION

A comparison of numerical and analytical solutions is provided using the solutions obtained in Equations (28) and (46) respectively. A discussion of results based on the simulations of the validated results obtained in

<http://www.ijesrt.com> © International Journal of Engineering Sciences & Research Technology

Equation (28) is also provided. Results are presented on the basis of effect of various Peclet numbers on pollutant concentration and effect of temporally varying velocity and dispersion coefficients with time on pollutant concentration.

3.1. Comparison of Analytical and Numerical Solutions

In this section, we compare the analytical and numerical solutions based on Equations (46) and (28) respectively. The simulations are obtained at a fixed time ($t^* = 1$) using $U_0 = 1.14, D_0 = 1.40 (Pe \sim 1)$. Both velocity and dispersion coefficients are considered as exponentially increasing with time.

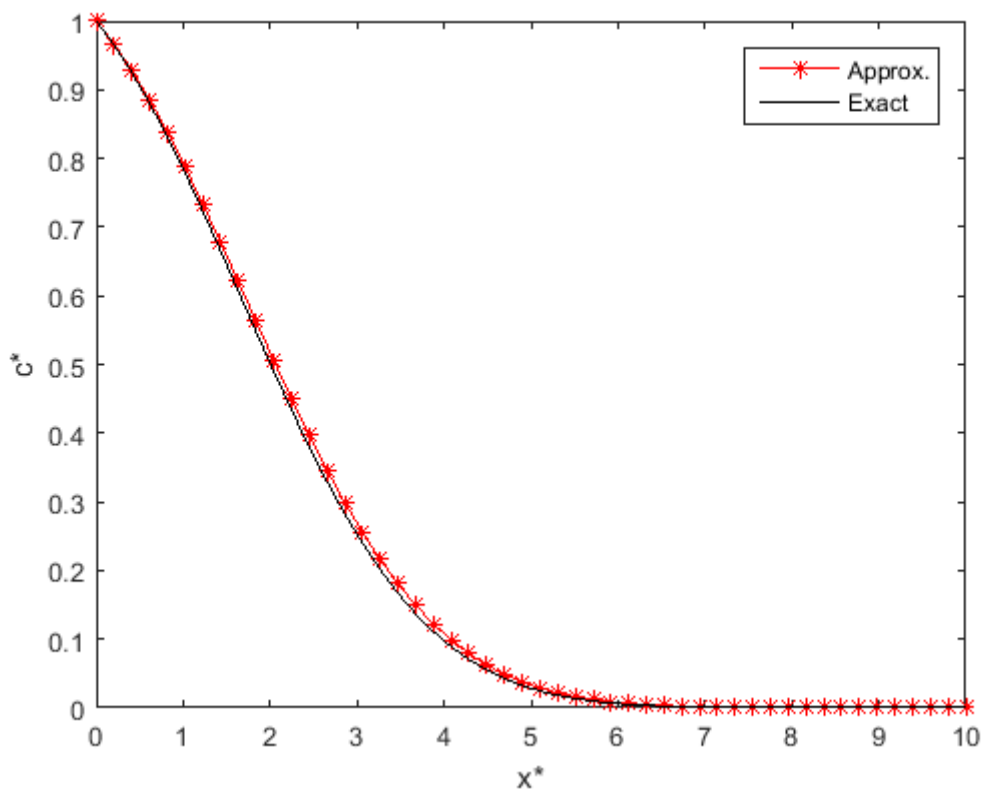


Figure 1: Plot of Analytical and Numerical Solutions of c^* against x^* when $t^* = 1$

Figure 1 shows concentration profile obtained when analytical (exact) and numerical (approximate) solutions are compared. Absolute error is evaluated using concentration values from both the exact (c_e^*) and approximate (c_a^*) solutions. The errors obtained at different points are summarized in Table 1:

Table 1: Comparison of Exact and Approximate Solutions

x^*	c_e^*	c_a^*	Absolute Error
1	0.77900	0.787800	8.8×10^{-3}
2	0.490400	0.506500	1.61×10^{-2}
3	0.239900	0.255700	1.98×10^{-2}
4	0.088890	0.098870	9.98×10^{-3}
5	0.024540	0.037690	1.315×10^{-2}
6	0.007038	0.007038	0.00
7 - 10	0.000000	0.000000	0.00

From Table 1 above, we observe that the numerical results obtained using FTCS agree with the analytical results to a great degree. We conclude that our scheme is accurate. Simulations obtained in our study are based on the numerical scheme.

3.2. Effect of Velocity and Dispersion on Pollutant Concentration

Both advection and diffusion processes move pollutants from one place to another, but each accomplishes this differently. Whereas advection transports pollutant molecules downstream, diffusion transports pollutant molecules in both ways regardless of the stream direction. In order to understand the effect of each process on pollutant concentration, a comparison of advection and diffusion fluxes is performed using the ratio of their scales. This ratio is given by Peclet number (Pe). Simulations are obtained for pollutant concentration when $Pe \ll 1$, $Pe \sim 1$ and $Pe \gg 1$.

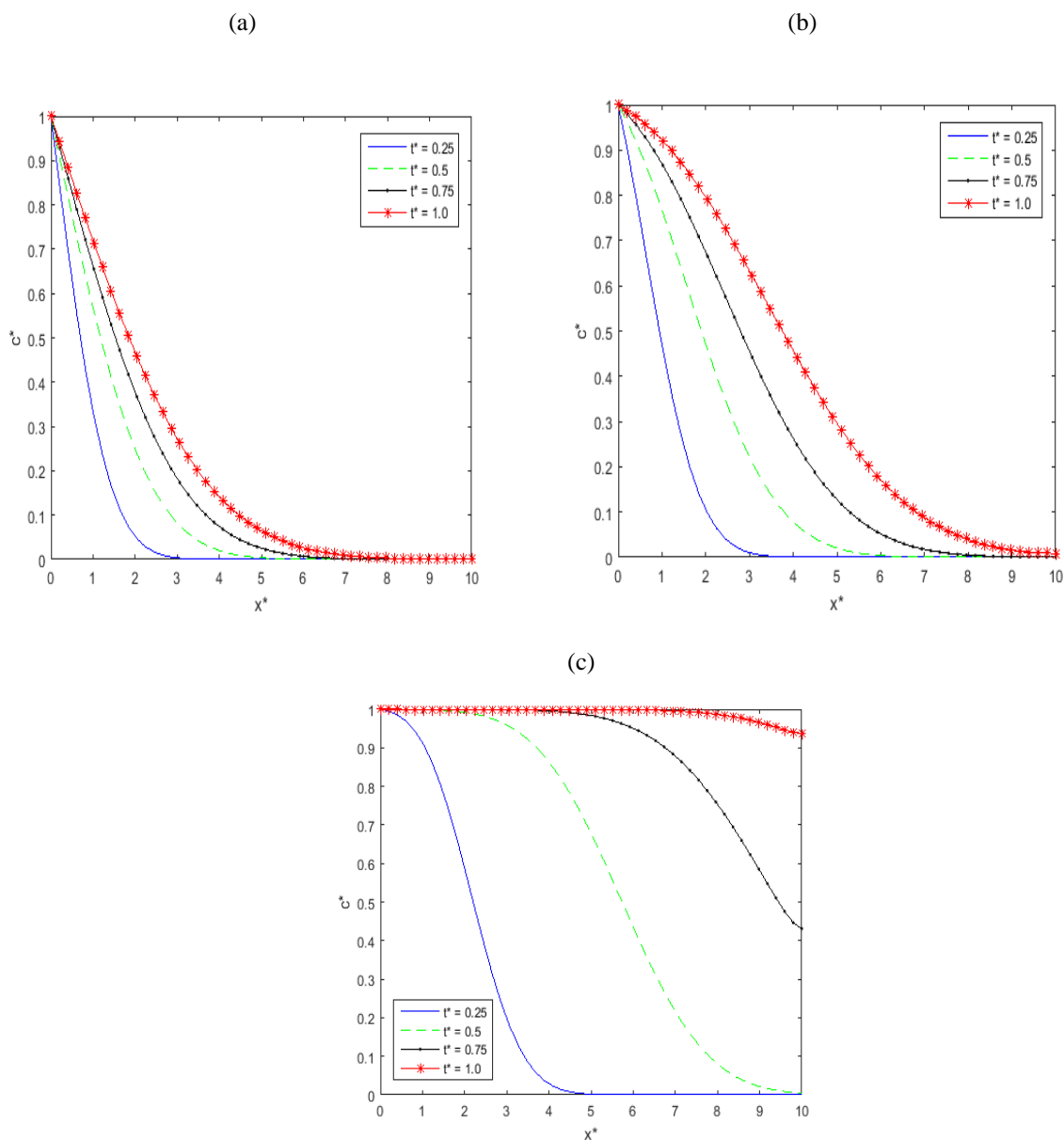


Figure 2: Plot of $c^*(x^*)$ for $t^* = 0.25, 0.5, 0.75$ and 1 for (a) $Pe \ll 1$ (b) $Pe \sim 1$ (c) $Pe \gg 1$

If $Pe \ll 1$, advection term is significantly smaller than diffusion term. The simulations are obtained using initial velocity and dispersion coefficients as $U_0 = 0.05, D_0 = 1.25$ respectively. We observe from Figure 2(a) that at a fixed point near the source ($x^* = 0$), concentration increases with increasing time. For example at $x^* = 2$, for $t^* = 0.25, c^* = 0.0472$; for $t^* = 0.5, c^* = 0.2393$; for $t^* = 0.75, c^* = 0.3673$ and for $t^* = 1, c^* = 0.4587$. Increase in concentration is as a result of increased spreading of pollutant cloud around the source. Pollutant cloud spreads in the medium faster than it is transported downstream. Concentration however becomes zero at some distance from the source. This is based on the assumption that pollutants being considered are miscible and there are no storage areas or dead zones in the river that would retain pollutants then release them after some time. We further observe that at any fixed time, concentration decreases with increasing distance. For example when $t^* = 0.5$, for $x^* = 1, c^* = 0.5594$; for $x^* = 2, c^* = 0.2393$; for $x^* = 3, c^* = 0.07609$; for $x^* = 4, c^* = 0.01765$; for $x^* = 5, c^* = 0.004327$; for $x^* = 6, c^* = 0.000551$ and for $x^* \geq 7, c^* \approx 0$. When $Pe \ll 1$, there is minimal spreading of pollutant molecules at some far distance from the source point thus less significant effect on the concentration at far distance.

When $Pe \sim 1$, the advection and diffusion terms are not significantly different and neither process dominates over the other. The results in Figure 2(b) are obtained using initial velocity and dispersion coefficients as $U_0 = 1.14, D_0 = 1.40$ respectively. We note that at $x^* = 2, t^* = 0.25, c^* = 0.0972$; for $t^* = 0.5, c^* = 0.4588$; for $t^* = 0.75, c^* = 0.6657$; and for $t^* = 1, c^* = 0.7943$. The high concentration levels around source point and gradual decrease of pollutant concentration thereafter is due to the fact that once a mass of pollutant is released at a single instant of time in the river, it spreads out as it moves downstream due to molecular diffusion caused by random motion of pollutant molecules, spreading caused by the variations of the microscopic velocities through the pores in the river and advection due to bulk movement of water. We also observe that for a fixed time, concentration decreases with increasing distance. For example, when $t^* = 0.5$: for $x^* = 1, c^* = 0.7616$, for $x^* = 2, c^* = 0.4588$; for $x^* = 3, c^* = 0.2096$, for $x^* = 4, c^* = 0.07062$; for $x^* = 5, c^* = 0.2346$; for $x^* = 6, c^* = 0.00379$, for $x^* = 7, c^* = 0.0005803$ and for $x^* \geq 8, c^* \approx 0$. Though concentration decreases with distance as we move downstream, concentration in this case at any point downstream is higher as compared to when $Pe \ll 1$, due to the effect of advection process during flow.

Simulations are further obtained using initial velocity and dispersion coefficients as $U_0 = 4, D_0 = 1.05$ respectively for $Pe \gg 1$. In this case, advection term is significantly bigger than the diffusion term. Results in Figure 2(c) show that at a fixed point near the source, concentration increases with increasing time and reaches a maximum value ($c^* = 1$) after a given time. For example at $x^* = 4$, for $t^* = 0.25, c^* = 0.02354$; for $t^* = 0.5, c^* = 0.8515$; for $t^* = 0.75, c^* = 0.9999$; and for $t^* = 1, c^* = 0.9999$. When advection dominates the flow, spreading is minimal with the cloud of pollutant being simply moved along by the flow. This is because the pollutant is transported downstream very first and has less time to spread. We also observe that for a fixed time, concentration decreases with increasing distance. For example, when $t^* = 0.5$: for $x^* = 1, c^* = 1$, for $x^* = 2, c^* = 1$, for $x^* = 3, c^* = 0.9553$, for $x^* = 4, c^* = 0.8515$; for $x^* = 5, c^* = 0.7009$; for $x^* = 6, c^* = 0.4553$, for $x^* = 7, c^* = 0.2273$, for $x^* = 8, c^* = 0.08369$, for $x^* = 9, c^* = 0.02209$, and for $x^* = 10, c^* = 0.005173$. Due to significant effect of the process of advection in transporting molecules downstream, we note that at any point, there are pollutant molecules present at downstream especially for $0.5 \leq t^* \leq 1$.

Comparison of pollutant concentration for different Peclet numbers across the domain $0 \leq x^* \leq 10$ at a fixed time ($t^* = 0.5$) is provided in Table 2:

Table 2: Table Showing Pollutant Concentration for Various x^* and Pe

x^*	$Pe \ll 1$	$Pe \sim 1$	$Pe \gg 1$
1	0.559400	0.761600	1.000000
2	0.239300	0.458800	1.000000
3	0.076090	0.209600	0.955300
4	0.017650	0.070620	0.851500
5	0.004327	0.023460	0.700900
6	0.000551	0.004379	0.455300

7	0.000000	0.000580	0.227300
8	0.000000	0.000000	0.083690
9	0.000000	0.000000	0.0220900
10	0.000000	0.000000	0.005173

Comparing the three cases of varying Peclet number, at a fixed time say $t^* = 0.5$, it is observed that at any point x^* , concentration is much higher for $Pe \gg 1$ as compared to when $Pe \ll 1$ and $Pe \sim 1$. When flow velocity is significantly higher than diffusion, more pollutant molecules are transported downstream faster than they are spread around the source point. The effect of bulk transport of pollutant molecules is also seen at the downstream for $Pe \gg 1$ where concentration is evident unlike the two cases where $Pe \ll 1$ and $Pe \sim 1$.

3.3. Effect of Temporally Varying Velocity and Dispersion Coefficients on Pollutant Concentration

To study the effect of time dependent dispersion ($D(t) = D_0 f_1(mt)$) and velocity coefficients ($U(t) = U_0 f_2(mt)$) on concentration, $f_i(mt)$ for $i = 1,2$ was considered to be an exponential function of time. Simulations were obtained at a fixed time ($t^* = 1$) using $Pe \sim 1$ for four different combinations of $f_i(mt)$ for $i = 1,2$.

Table 3: Summary of Different Combinations of $f_i(mt)$; $i = 1, 2$

$f_1(mt)$	$f_2(mt)$	Description of dispersion $D(t) = D_0 f_1(mt)$ in a flow of velocity $u(t) = U_0 f_2(mt)$
e^{mt}	e^{mt}	Exponentially increasing dispersion in an exponentially accelerating flow
e^{mt}	e^{-mt}	Exponentially increasing dispersion in an exponentially decelerating flow
e^{-mt}	e^{mt}	Exponentially decreasing dispersion in an exponentially accelerating flow
e^{-mt}	e^{-mt}	Exponentially decreasing dispersion in an exponentially decelerating flow

Simulation obtained for various time dependent advection and diffusion coefficients given in Table 3 are provided in Figure 3:

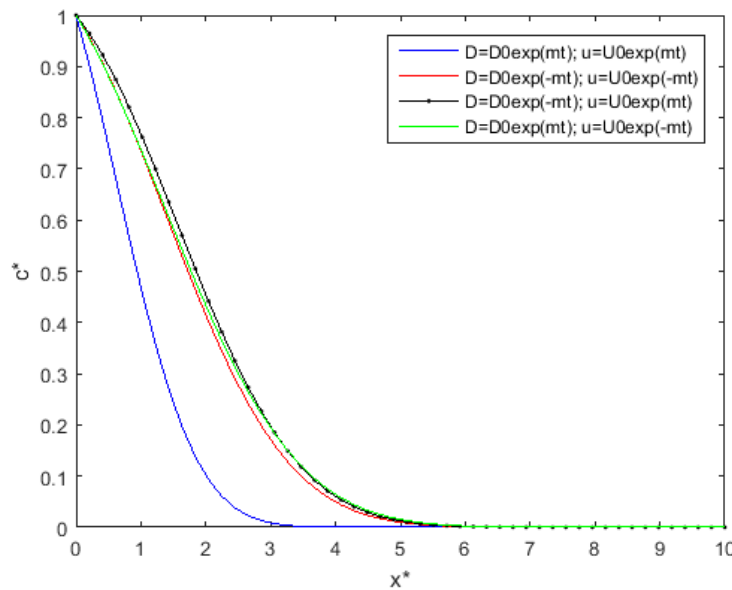


Figure 3: Plot of c^* against x^* when $t^* = 1$, for Different Time Dependent Diffusion and Velocity Coefficients

It is observed that at any fixed point, concentration is lower when both velocity and dispersion coefficients are exponentially increasing with time. For example, when $x = 2$, $c^* = 0.09349$. When both flow velocity and dispersion parameters are increasing with time, there is rapid mixing of pollutants after injection and immediate transportation of pollutants downstream occur simultaneously such that very few pollutant molecules are left around the source point in the shortest time possible. Concentration is however found to be higher when both velocity and dispersion coefficients are exponentially decreasing with time, ($x = 2$, $c^* = 0.4026$) as compared to the former case. This would be attributed to accumulation of pollutant molecules within the medium since spreading and transportation processes takes place at a much slower rate. There is no significant difference in concentration obtained when an exponentially decreasing dispersion in an exponentially decelerating flow ($x = 2$, $c^* = 0.4226$) is compared to that of exponentially increasing dispersion in an exponentially decelerating flow ($x = 2$, $c^* = 0.4217$). It is further observed that concentration is highest ($x = 2$; $c^* = 0.4420$) when we have exponentially decreasing dispersion in an exponentially accelerating flow. Again, because of less dispersion effect there tends to be increased accumulation of pollutant molecules.

4. CONCLUSION

We have noted that concentration generally increases around the source point and gradually decreases with increasing distance from the source point. At some far point from source, the concentration values converge to very small positive constant, almost zero. This implies that if we manage to maintain low pollutant levels at source point then the water downstream will be safe for human consumption. The simulations generally show skewness in the longitudinal distribution of the concentration with the average concentration being more downstream to the original source. The skewness is as a result of imbalance between the advective and dispersive processes. When varying Peclet numbers, we note that concentration is highest for $Pe \gg 1$. Physically, $Pe \gg 1$ represents surface waters in mountain regions, where the stream/ river is characterized by large velocities which makes advection more significant while $Pe \ll 1$ represents surface waters in plain areas where advection is characterized by smaller velocities. The results can be applied in many physical situations described by advection diffusion phenomena to help in the planning and management of rivers flowing through cities.

5. ACKNOWLEDGEMENTS

This work is part of the thesis done by the first author towards her doctoral studies. We acknowledge the Technical University of Kenya for the financial support in terms of tuition waiver to the first author.

REFERENCES

1. Ahmed S.G., "A Numerical Algorithm for Solving Advection Diffusion Equation with Constant and Variable Coefficients," in Open Numerical Method Journal. Vol. 4, pp. 1 - 7, 2012.
2. Alebrahim J., "Forward Time Centered Space Scheme for the Solution of Transport Equation," in International Annals of Science. Vol. 2, No. 1, pp. 1 – 5, 2017.
3. Andallah L.S. and Khatun M.R., "Numerical Solution of Advection Diffusion Equation using Finite Difference," in Bangladesh Journal of Industrial Research. Vol. 55, No.1, pp. 15 - 22, 2020.
4. Appadu, A.R., "Numerical Solution of the 1D Advection Diffusion Equation using Standard and Non Standard Finite Difference Scheme," in Journal of Applied Maths. ID 734374, 2013.
5. Duffy, D.G., "Green's Function with Applications," in Chapman and Hall/CRC, 2001.
6. Gurarslan G, Sari M and Zeytinoglu A., "Higher Order Finite Difference Schemes for Solving the Advection Diffusion Equation," in Mathematical Modeling and Computational Applications, Vol. 15, No.3, pp. 449 – 460, 2010.
7. Huang K, Simunek J and Genuchten M.T.H., "A Third Order Numerical Scheme with Upwind Weighting for Solving the Solute Transport Equation" in International Journal for Numerical Methods in Engineering," Vol. 40, pp. 1623 – 37, 1997.
8. Johari, H., Rusli, N. and Yahya, Z. "Finite Difference Formulation for the Prediction of Water Pollution," in IOP Conf. Series: Materials Science and Engineering. Vol. 318, 012005. 2018.
9. Kumar, A., Kumar, D.J, and Kumar, R.R., "Analytical Solutions to the One - Dimensional Advection Diffusion Equation with Time Dependent Coefficients," in Journal of Water Resources and Protection. Vol. 3, pp. 76 - 84, 2011.



10. Kaya, B. and Gharehbaghi, “Implicit Solutions of Advection Diffusion Equation by Various Numerical Methods,” in Australian Journal of Basic and Applied Sciences. Vol. 8, No.1, pp. 381 - 391, 2014.
11. Manitcharoen, N. and Pimpunchat, B., “Analytical and Numerical Solutions of Pollution Concentration with Uniformly and Exponentially Increasing Forms of Sources,” in Journal of Applied Mathematics. 9 pages. Article ID 95, 2020.
12. Van Genuchten, M. Th., and Alves, W.J., “Analytical Solutions of the One Dimensional Convective – Dispersive Solute Transport Equation,” in U.S. Department of Agriculture, Technical Bulletin. No. 1661, 1982.
13. Yip, B.F., Alias, N.A.F and Kasiman, E.H., “Numerical Modeling of Pollutant Transport in a Straight Narrow Channel using Upwind Finite Difference Method,” in IOP Conf. Series: Materials Science and Engineering. 1153,012003, 2021.

